FEBS 17139

FEBS Letters 388 (1996) 103–111

Two-dimensional crystallization of rabbit C-reactive protein on lipid monolayers

Sen-fang Sui[a,*], Zheng Liu[a], Wei Li[a], Caide Xiao[a], Shaoxiong Wang[a], Qiufeng Gao[b], Qingzhong Zhou[b]

[a]*State Key Laboratory of Biomembrane and Membrane Biotechnology, Department of Biological Sciences and Biotechnology, Tsinghua University, Beijing 100084, China*

[b]*College of Chemistry and Molecular Engineering, Peking University, Beijing 100871, China*

Received 4 March 1996; revised version received 10 May 1996

Abstract Two-dimensional (2D) crystals of rabbit C-reactive protein (CRP) have been obtained by protein binding on lipid monolayers at the air/water interface. Two different types of crystalline arrays of CRP were obtained, by specific binding and non-specific adsorption to the lipids. Electron crystallographic analysis of the negatively stained specimens showed that the unit cell parameters of the CRP 2D crystals formed by specific binding were a = 81 Å, b = 78 Å, γ = 118.35°, and those formed by non-specific adsorption were a = 74 Å, b = 67 Å, γ = 95.5°, both with the layer group p1. Projection maps were obtained at a resolution of 26 Å and 22 Å respectively. They showed that only the monomers of the CRP were packed in the 2D arrays and the orientations of the monomers on the lipid monolayers were different in the two types of crystals. By comparing the two projection maps, a preliminary shape of the CRP monomer has been derived. A model of the pentameric structure of the oligomeric CRP has been proposed.

Key words: C-reactive protein; Two-dimensional crystallization of protein; Electron crystallographic analysis; Molecular assembly; Lipid monolayer

1. Introduction

C-reactive protein (CRP) is one of the most characteristic acute phase proteins in man and in many other animals. The discovery of human CRP was made originally by Tillett and Francis [1]. Its expression level in the blood is increased 1000-fold from trace amounts (about 100 ng/ml) during the first 24 h of a systemic inflammatory response [2,3]. CRP has been found on necrotic cells at sites of inflammation. Its binding can initiate the classical C pathway [4,5], optimize the phagocytosis [6], influence the activities of platelets and lymphocytes [7–9] and may thus contribute to inflammatory reactions.

CRP is a Ca^{2+}-dependent non-antibody precipitum with the C-polysaccharide of the pneumococcal cell wall or with cell membrane phospholipids [1,10]. This reactivity of CRP has been shown to be specific for the phosphorylcholine group in C-polysaccharide and lipid membrane [11]. The association constant of CRP with phosphocholine is about 10^7 M^{-1}. It also binds specifically to a variety of other organic phosphate esters, such as monophosphate and phosphorylethanolamine, particularly to phosphorylcholine [11–13].

CRP is composed of five identical non-covalently linked monomers arranged in a planar ring with pentameric symmetry [14]. Each monomer has 206 amino acids and a molecular weight of about 21 kDa. It has one binding site for phosphate esters with a high affinity for the phosphocholine group and at least two binding sites for calcium ions. The amino acid sequence of the protein was first determined by amino acid sequencing [15] and later confirmed by cDNA sequencing [16,17]. The amino acids within the proposed phosphocholine binding site are conserved among all the known CRP sequences from *Limulus* through mammals [18]. Several mouse anti-idiotype monoclonal antibodies, directed against the idiotype present within the phosphocholine-binding region of mouse antibodies, also recognize the phosphocholine-binding region of human CRP [19,20]. Thus the Ca^{2+}-dependent phosphocholine-binding activity is considered a common functional characteristic of CRP from all species [21].

In order to study the functional mechanism of CRP at a molecular level, a three-dimensional structure of the protein must be determined. The three-dimensional crystals suitable for X-ray diffraction of CRP from *Limulus polyphemus* [22], from rat [23] and from man [24,25] have been grown, but a detailed structure has not been reported. Two-dimensional crystals of macromolecules are particularly suitable for structure determination by electron crystallographic analysis [26]. A general method of 2D crystallization based on the interactions between soluble proteins and ligand-containing lipid layers has been developed by Kornberg and his co-workers [27,28] and has been applied successfully in many cases [29–38]. In the present paper, we report two forms of 2D crystals of rabbit CRP grown on lipid monolayers at the air/water interface under two different conditions based on the specific binding and non-specific electrostatic adsorption of protein with lipid monolayers. Electron microscopic analysis has been done on these crystal forms and projection maps have been calculated. Additional structural information on CRP was obtained by comparing the two projection maps of the two type 2D crystals.

2. Materials and methods

2.1. Materials

DMPC, DMPE, DMPS, DPPC, DPPE, DOPC, DOPE, Sepharose 4B, phosphorylethanolamine-Sepharose 4B, sheep anti-human CRP antibody were products from SIGMA. C-polysaccharide was isolated from the pneumococcal cell wall according to Anderson and McCarty [39].

*Corresponding author. Fax: (86) (10) 62568182.
E-mail: dbsssf@tsinghua.edu.cn

Abbreviations: 2D, two-dimensional; CRP, C-reactive protein; DMPC, dimyristoyl phosphatidylcholine; MPE, dimyristoyl phosphatidylethanolamine; DMPS, dimyristoyl phosphatidylserine; DOPC, dioleoyl phosphatidylcholine; DOPE, dioleoyl phosphatidylethanolamine; DPPC, dipalmitoyl phosphatidylcholine; DPPE, dipalmitoyl phosphatidylethanolamine; DS8PE, dioctadecanyl *N*-[*N'*-(aminoethyl phosphatoethyl) succinamido-*N*-yl]-aspartate inner salt

PII S0014-5793(96)00528-5

2.2. Purification of rabbit C-reactive protein

Rabbit CRP was purified from the acute phase serum of white rabbits by affinity chromatography on phosphorylethanolamine-Sepharose 4B according to the published procedure [40]. Briefly, rabbit was injected intramuscularly with turpentine (0.5 ml/kg), 36 h prior to the withdrawal of the blood. The serum was passed through an affinity column of phosphorylethanolamine-Sepharose 4B, which had been equilibrated with TBS-Ca^{2+} buffer (0.02 M Tris-HCl, 0.15 M NaCl, 10 mM $CaCl_2$, pH 7.8), in the presence of Ca^{2+} (10 mM). The bound CRP was eluted using 1.15 M NaCl in TBS-Ca^{2+} buffer, the fractions containing other proteins were pooled. After washing the column with TBS-Ca^{2+} buffer, the CRP was eluted with 0.1 M phosphorylcholine chloride in TBS-Ca^{2+} buffer. The fraction then passed rapidly through a Sepharose 4B column (equilibrated with TBS-Ca^{2+} buffer) to remove serum amyloid P-component. The eluted protein was dialysed against TBS-Ca^{2+} buffer and then against TBS-EDTA (0.02 M Tris-HCl, 0.15 M NaCl, 10 mM EDTA, pH 7.8) to dissociate any bound phosphorylcholine and Ca^{2+}. The solution was then dialysed against pure water to remove the other ions. The CRP concentration was measured by absorbance at 280 nm ($E_{1\%}$=20.3 cm^{-1}). Polyacrylamide gel electrophoresis in the presence of sodium dodecyl sulfate of CRP prepared in this way showed a single protein band with a molecular weight of 20 kDa (corresponding to one CRP monomer). The reactivity of the purified CRP was examined by immunoprecipitation with C-polysaccharide and with sheep anti human CRP antibodies.

2.3. Preparation of the synthetic lipid DS8PE

When CRP purification is performed using affinity chromatography, phosphorylethanomine is linked to the agarose bead through a long-arm chain. Inspired by this method, in this work we used a home-synthesized lipid [41] with a long-arm spacer between the polar head group and the hydrophobic tails as the membrane bound lipid ligand of CRP. The structure of the synthesized lipid is shown in Fig. 1. The chemical reactions to prepare this synthetic lipid are also displayed schematically in Fig. 1 which partly follows the work of Eibl and his co-workers [42,43]. It is dioctadecanyl *N*-[*N'*-(aminoethyl phosphatoethyl)-succinamido-*N*-yl]-aspartate inner salt. We have abbreviated it to DS8PE, 'DS' stands for the 18 carbon hydrophobic tails, 'PE' for the polar head group, and '8' means the insert 8-atom chain as a spacer. The inserted spacer between the tails and the head group may make the head groups stretch out of the membrane surface.

2.4. 2D crystallization

2D crystals were obtained using the lipid monolayer technique with small Teflon wells (4 mm in diameter and 0.5 mm in depth) [28]. In general, a solution of protein was placed in the wells first. The lipid sample in solvent was then spread on the surface of protein solution. The protein molecules concentrated at the surface of the monolayers because of the specific binding to the special lipid ligands or the electrostatic adsorption to the charged lipids. The fluidity of the lipid monolayers allowed the molecules to arrange themselves laterally into two-dimensional ordered arrays.

In our experiments, droplets (~15 μl) of CRP solution were placed in Teflon wells, and the surface of the droplets coated with 0.5–1 μl of lipid mixture of different lipids in chloroform/methanol (3:1, v/v) at different molar ratios. The protein solution contained 50–200 μg/ml CRP in 5 mM $CaCl_2$, 20 mM Tris-HCl, 100 mM NaCl, at pH 6.8. Incubations were carried out at 25°C for 48 h. The Teflon wells were always sealed in a humid chamber to reduce evaporation.

The amount of lipid sample added to each well was much more than that required to form a monolayer. Thus, the lipid membrane was assumed to be in the highest pressure state that it could reach. This assumption was supported by control experiments completed in a well with a larger surface (diameter 50 mm). The maximal surface pressure in the control experiments was obtained about 40 mN/m (see Fig. 2). The lipid packing density is an important factor in growing crystals, however it is hard to calculate the lipid density in the 4 mm diameter well directly from the initial lipid amount because of the 'edge' effect [44,45].

2.5. Electron microscopy and image processing

After incubation in the small well, the lipid monolayers with ordered protein patches were first picked up on carbon-coated electron microscopic grids in a Langmuir-Schaefer type of transfer [46]. In this technique, the spread monolayer film was transferred to the substrate which was parallel to the air-water interface. Then the grids were washed with one droplet of distilled water, and then negatively stained with 1% (w/v) uranyl acetate for 30–60 s.

The negatively stained samples were examined in a Hitachi H-800 transmission electron microscope. The quality of the images and the crystalline order of CRP were evaluated by optical diffraction. The best images were used for further analysis by computer after digitization. The numeric images were processed using the MRC image processing package [26]. The lattice vectors (a^* and b^*) of the diffraction pattern were refined by the coordinates of the visible peaks. Then the whole diffraction was filtered according to the refined vectors (a^* and b^*), and the values of amplitude and phase were extracted by program MMBOX. The signal-to-noise ratio of each peak was evaluated by IQ value [47]. In this work, only peaks with IQ less than 7 were used in final Fourier synthesis.

3. Results

3.1. Two-dimensional crystallization of CRP induced by specific binding

DS8PE has been used as the lipid ligand of CRP at the air/water interface in the present work, thus CRP can bind specifically onto the DS8PE-containing lipid monolayers. The lipid mixtures at different ratios of DS8PE/DOPC, DS8PE/DOPE, DS8PE/DPPE and DS8PE/DPPC have been used to investigate the effects of lipids on the 2D crystallization of the C-reactive protein. Some pure natural lipids, such as DMPC, DMPE, DPPC, DPPE, DOPC and DOPE were also tried. However, 2D crystals were only observed with monolayers of DS8PE/DOPC and DS8PE/DOPE.

Fig. 3A shows an electron micrograph of a negatively stained 2D crystal of CRP on DS8PE/DOPC (1:20) monolayer. The size of this crystal area is about 0.25×0.34 μm. The computed diffraction pattern (shown in Fig. 3B) reveals that the crystal has an average unit cell a=81 Å, b=78 Å, and γ=118.35°. The (3,1) reflection is visible by eye (marked with an arrow in Fig. 3B), corresponding to 26 Å resolution. The projection electron density map is shown in Fig. 3C. It can be estimated from the shape of the high-density region and the size of the unit cell that there is only one monomer of CRP per unit cell. The contour of the individual monomer is similar to a trapezoid. The length of the top side of the trapezoid is about 20 Å, and that of the bottom is about 45 Å, and the height is about 60 Å. The highest density region marked with ★ in Fig. 3C is located in the near central of the monomer, which is about 20 Å from this region to the bottom of the trapezoid.

Within the limits of error, the diffraction pattern of the crystals seems to have a hexagonal symmetry, but by analyzing the phases of the diffraction spots, we could find no 2-, 3- or 6-fold symmetry in this specimen. This can also be demonstrated by the final projection maps.

3.2. Two-dimensional crystallization of CRP induced by non-specific adsorption

As mentioned above, CRP can form 2D crystals on DS8PE-containing lipid monolayers based on the specific binding between CRP and its lipid ligands. Another kind of lipid mixture, DMPS-containing lipid monolayers, was also used for CRP 2D crystallization, which is based on the electrostatic adsorption of protein in solution to the lipid monolayers.

Under normal conditions, DMPS is a negatively charged

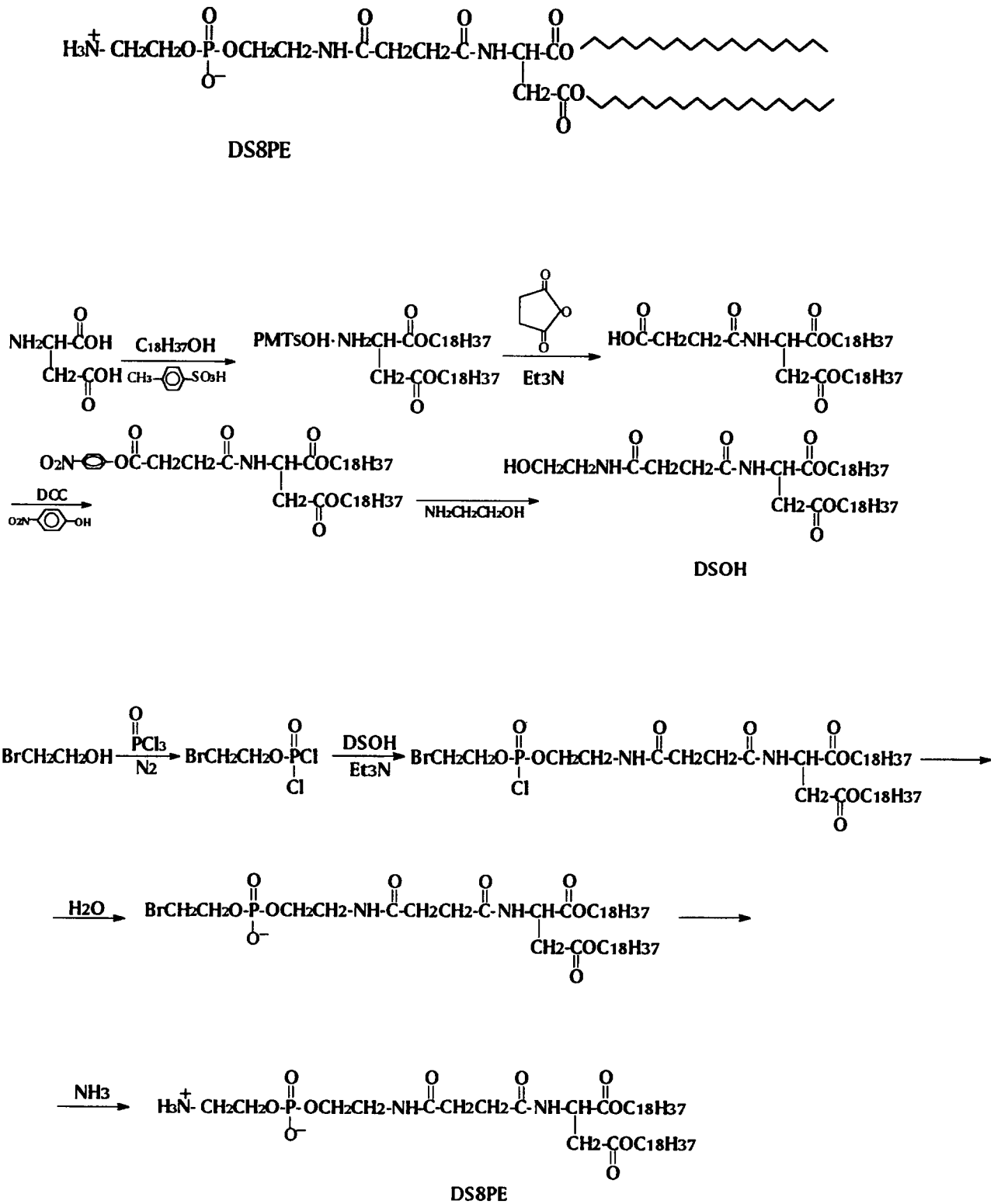

Fig. 1. The molecular structure of the synthetic lipid DS8PE and the scheme of the preparation process.

lipid. The isoelectric point of CRP is pH5.5, when the pH is below 5.5, CRP is positively charged. Thus CRP can non-specifically adsorb by electrostatic interactions and be concentrated onto the DMPS-containing lipid monolayers.

Fig. 4A shows an electron micrograph of the negatively stained 2D crystal domain of CRP on DMPS/DOPE (1:5) monolayer. This crystal area is about 0.32×0.60 μm. The computed diffraction pattern (Fig. 4B) of the CRP 2D crystal shows a unit cell $a = 74$ Å, $b = 67$ Å, and $\gamma = 95.5°$. The (0,3) reflection is visible by eye (marked with an arrow in Fig. 4B), corresponding to 22 Å resolution. The projection electron density map is shown in Fig. 4C. In this map, two monomers

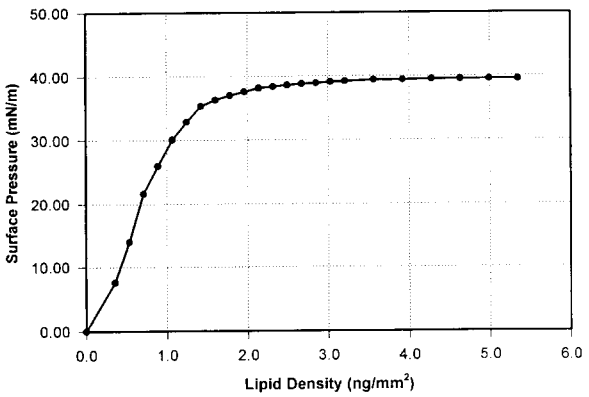

Fig. 2. Surface pressure characteristics of the DS8PE/DOPC monolayer. The Teflon well was in larger size (diameter 50 mm), and the surface pressure was measured by the Wilhelmy method. The subphase contained 100 μg/ml CRP, 5 mM $CaCl_2$, 20 mM Tris-HCl, 100 mM NaCl, pH 6.8. 0.5 μl of a well mixed solution of DS8PE/DOPC (1:20 molar ratio, total lipid concentration 0.7 μg/ml) was added onto the air/water interface at each time. After about 10 min for equilibrium, the surface pressure was recorded, all experiments were performed at 25°C. The plot demonstrates that the maximal surface pressure of the saturation stage of the DS8PE/DOPC monolayer was about 40 mN/m, and the minimal quantity required was about 2.3 ng/mm^2.

of CRP are vertically arranged (dot-line frames). The shape of the individual monomer is an ellipse. The long axis of the ellipse is about 60 Å, the minor axis is about 35 Å and the density distribution varies in the ellipse. In the region of the large end of the ellipse the density distribution is more compact than that in the region of the small end. In the center of the large end, there is also a high density region (marked also with ★ in Fig. 4C), which is about 20 Å from this region to the extreme of the large end.

4. Discussion

Although the phosphocholine group is the head group of major membrane phospholipids, CRP can not bind to the normal cell membrane. Volanakis and his co-workers studied the binding features of CRP to egg-phosphatidylcholine liposomes [48], and concluded that in intact phosphatidylcholine bilayers the polar head groups are not freely accessible to the binding site of CRP. We considered these phenomena may be the effect of the steric hindrance, and the phosphocholine-binding sites may be buried in the core of the proteins, and a long-arm spacer between the polar head group and the hydrophobic tail should be required to make the polar head group accessible to the binding site in the protein core. In present work, we synthesized DS8PE as the lipid ligand of

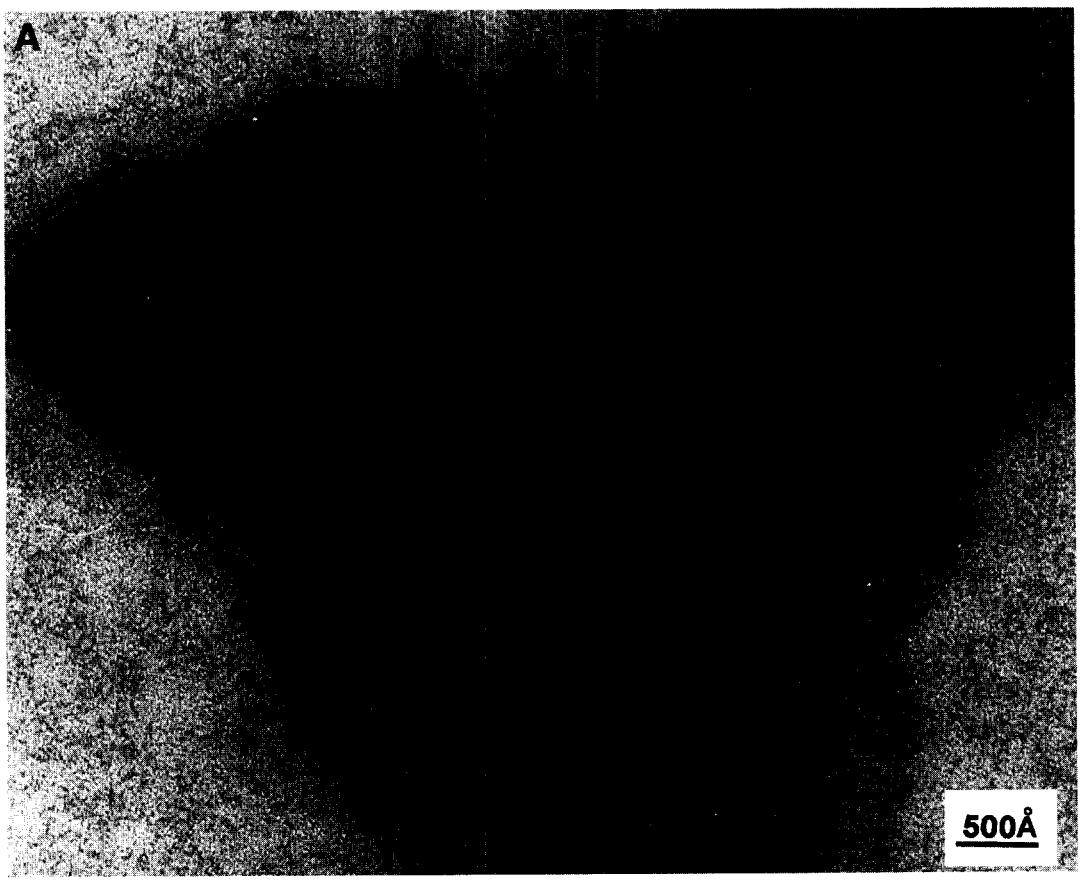

Fig. 3. Electron micrograph of the 2D crystal of CRP formed by specific binding on DS8PE/DOPC (1:20) monolayer and the projection map of the crystal. In preparing 2D crystals, the subphase contained 100 μg/ml CRP, 5 mM $CaCl_2$, 20 mM Tris-HCl, 100 mM NaCl, pH 6.8. 0.5 μl of a well mixed solution of DS8PE/DOPC (1:20, molar ratio) was added onto the air/water interface. Incubations were performed at 25°C for about 48 h. (A) Electron micrograph of a negatively stained specimen. It was taken at 80000× with an operation voltage of 100 kV. (B) The computed diffraction pattern. The (3,1) reflection, at 1/26 Å, is indicated by an arrow. (C) The projection map of CRP 2D crystals formed by specific binding, an area of 4×4 units of cells is shown.

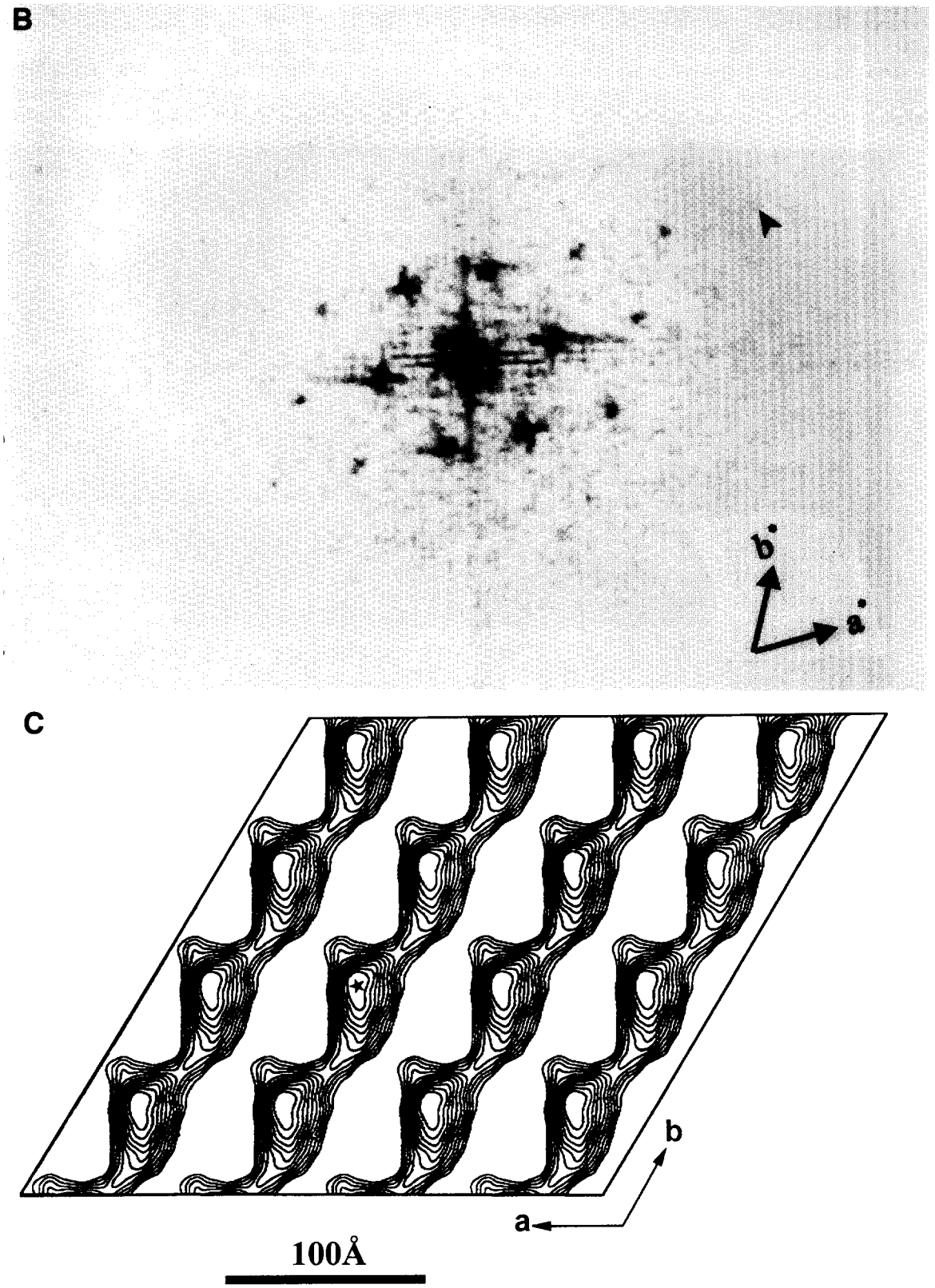

Fig. 3 (*continued*).

CRP, and obtained the 2D crystals of CRP on the DS8PE containing lipid monolayers.

It is believed that the fluidity of the lipid monolayer is a crucial factor for 2D crystallization by the lipid monolayer technique. As our experiments showed, for both the specific binding and the non-specific adsorption methods, an unsaturated lipid (DOPC or DOPE) was required to form 2D crystals. The double bond in the fatty chains could make the

monolayers more fluid, thus the membrane bound CRP would retain its lateral mobility on the monolayers availing rearrangement to form 2D crystals. Moreover, in the specific binding method, the unsaturated lipids were also used as a dilution lipid to increase the lateral distance between the head groups of DS8PE and overcome the lateral steric hindrance that restricts the CRP binding.

In the non-specific adsorption method, the pH value of the protein solution is another important parameter that affects 2D crystallization. DMPS is a lipid with negatively charged

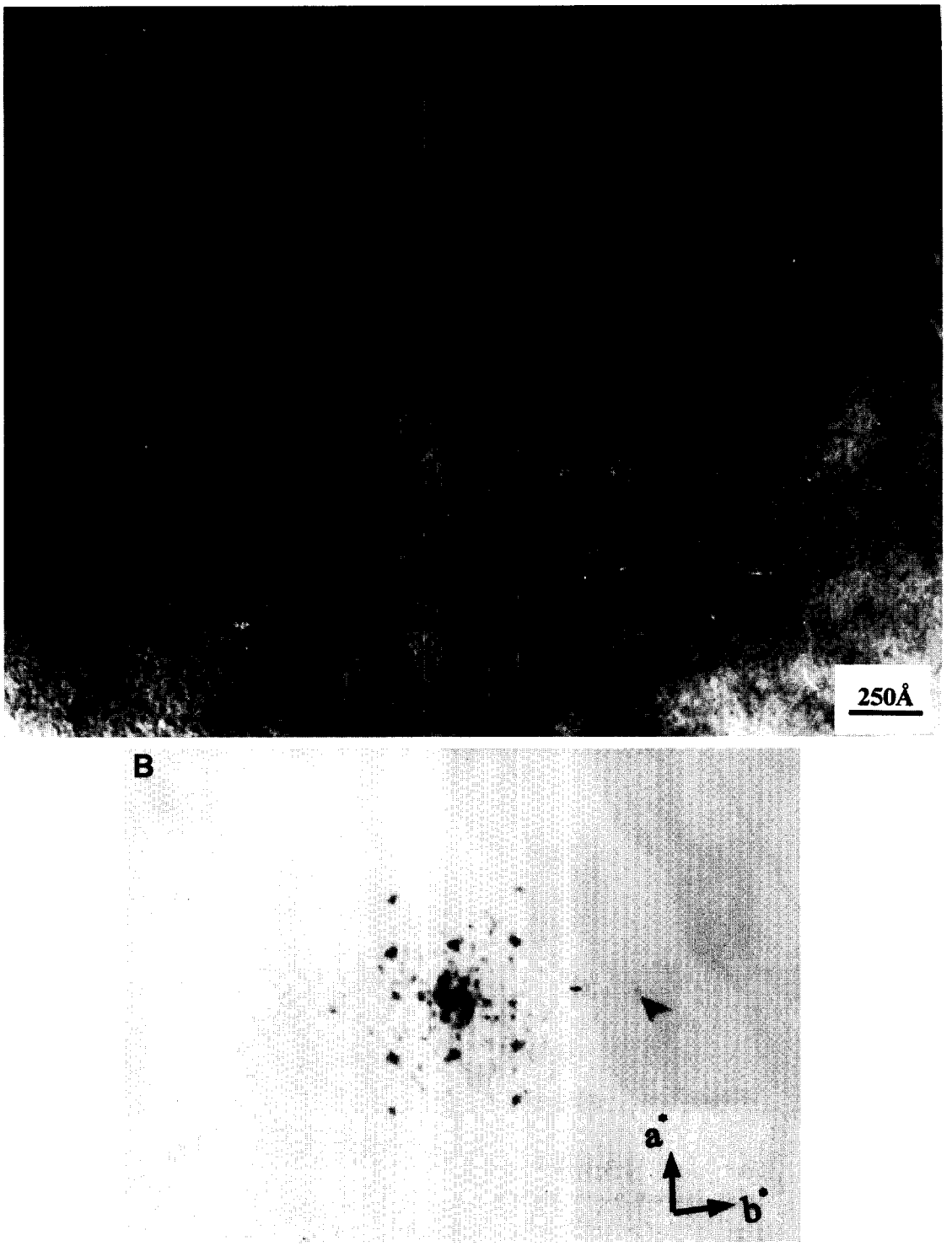

Fig. 4. Electron micrograph of the 2D crystal of CRP formed by non-specific adsorption on DMPS/DOPC (1:5) monolayer and the project map of the crystal. In preparing 2D crystals, the subphase contained 200 μg/ml CRP, 1 mM $CaCl_2$, 10 mM Tris-HCl, pH 4.5. 0.5 μl of a well mixed solution of DMPS/DOPC (1:5, molar ratio) was added onto the air/water interface. Incubations were performed at 25°C for about 48 h. (A) Electron micrograph of a negatively stained specimen. It was taken at 105000× with an operation voltage of 100 kV. (B) The computed diffraction pattern. The (0,3) reflection, at 1/22 Å is indicated by an arrow. (C) The projection map of CRP 2D crystals formed by non-specific adsorption, an area of 3×3 units of cells is shown.

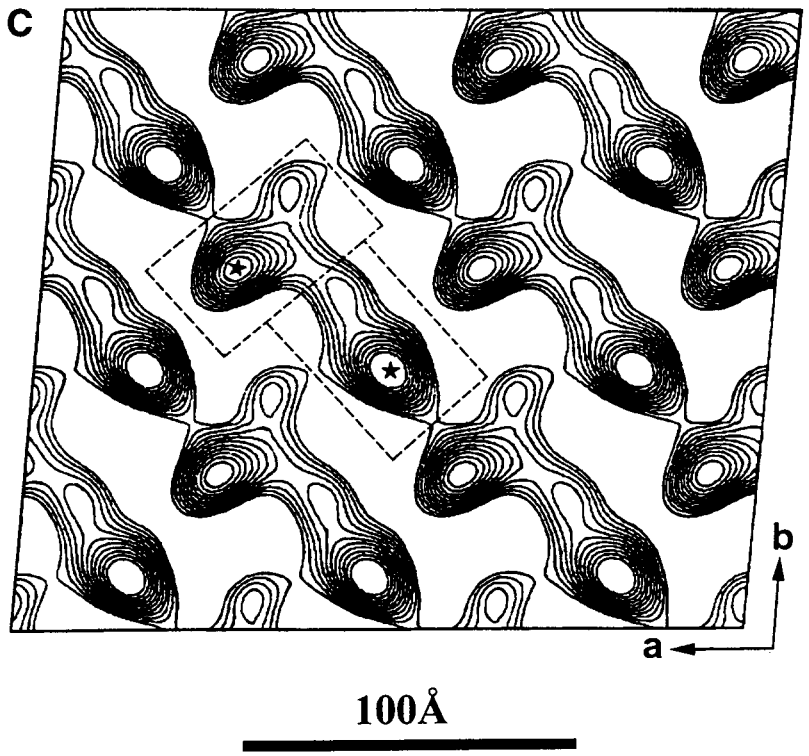

Fig. 4 (*continued*).

heads, while the charged characteristic of CRP is dependent upon the pH value of the solution. It is hard to find out any protein domain on the DMPS-containing lipid monolayers under neutral pH, since CRP is also negatively charged under neutral pH (pI of CRP is 5.5).

When examining the filtered image map of the CRP 2D crystals obtained by using the non-specific adsorption method (shown in Fig. 4C), we can see that the two monomers in one unit cell appear to be a screw axis running along the Y direction of the unit cell, and in the diffraction pattern (Fig. 4B), the (0,1) reflection is very weak. These would suggest the crystal to have pg symmetry. However, after we examined four crystals obtained by the same methods, we got a final result of the unit cell angle $\gamma = 95.5 \pm 2°$, we therefore believe that there is no pg symmetry in this type of crystals, and the layer group of the crystal is p1.

When examined under electron microscopy, as we mentioned above, only monomers of CRP existed in 2D crystalline arrays on the lipid monolayers, and occasionally some dispersed individual oligomeric CRP molecules were observed. As shown in Fig. 5A the dispersed oligomeric CRP displayed an ring-like shape. The diameter of the ring is about 120–140 Å. These results are in agreement with that of Osmand's work [14]. In Fig. 5A we can see also that in the center of the ring there is a stain-filled region, and the diameter of this region is about 30–40 Å.

In each monomer of CRP there is one binding site for phosphate esters with high affinity for the phosphocholine group. Using immunoelectron microscopy, the monoclonal antibodies to intact CRP that block phosphocholine binding have been shown to bind to the same position on each of the five monomers, and the monoclonal antibody binding sites were on only one of the planar surfaces of the pentameric ring [49]. When CRP specifically binds onto the lipid monolayers, the phosphocholine-binding sites should be facing towards the monolayers, thus the monomers of CRP are standing on one side of the planar surfaces of the ring on the lipid monolayers.

In Osmand's work [14], they also showed that the average thickness of an individual rabbit CRP molecule viewed from the side is 38 Å. This side-viewed width is identical with the length of the minor axis of the CRP monomers of which the 2D crystals were formed by non-specific adsorption. So this observation suggests that the CRP monomers of the 2D crystals formed by non-specific adsorption were standing on edge on the lipid monolayers, and the edge should be rich in positively charged amino acids so as to interact with the negatively charged lipid monolayers. There are two monomers of CRP per one unit cell (Fig. 4C), we suggest one monomer would face 'up' and the other 'down', this is consistent with the appearance of Fig. 4C, one monomer of which seems to curve to the left and the others to the right, thus both edges of the CRP monomers should be positively charged to perform a non-specific, charge-induced adsorption to the lipid monolayers.

When comparing the two projection maps of the CRP 2D crystals obtained by the two different methods, we can see that their outlines are quite different. This indicates that these two projection maps are obtained in different projection directions, and that the orientations of the monomers onto the lipid monolayers are different. As we mentioned above, the monomers in the 2D crystals formed by non-specific adsorption stand on edge while the monomers in specific binding-induced 2D crystals stand on one side of the planar surfaces with the phosphocholine-binding site towards the lipid monolayers. Thus the projection structure of the monomers in spe-

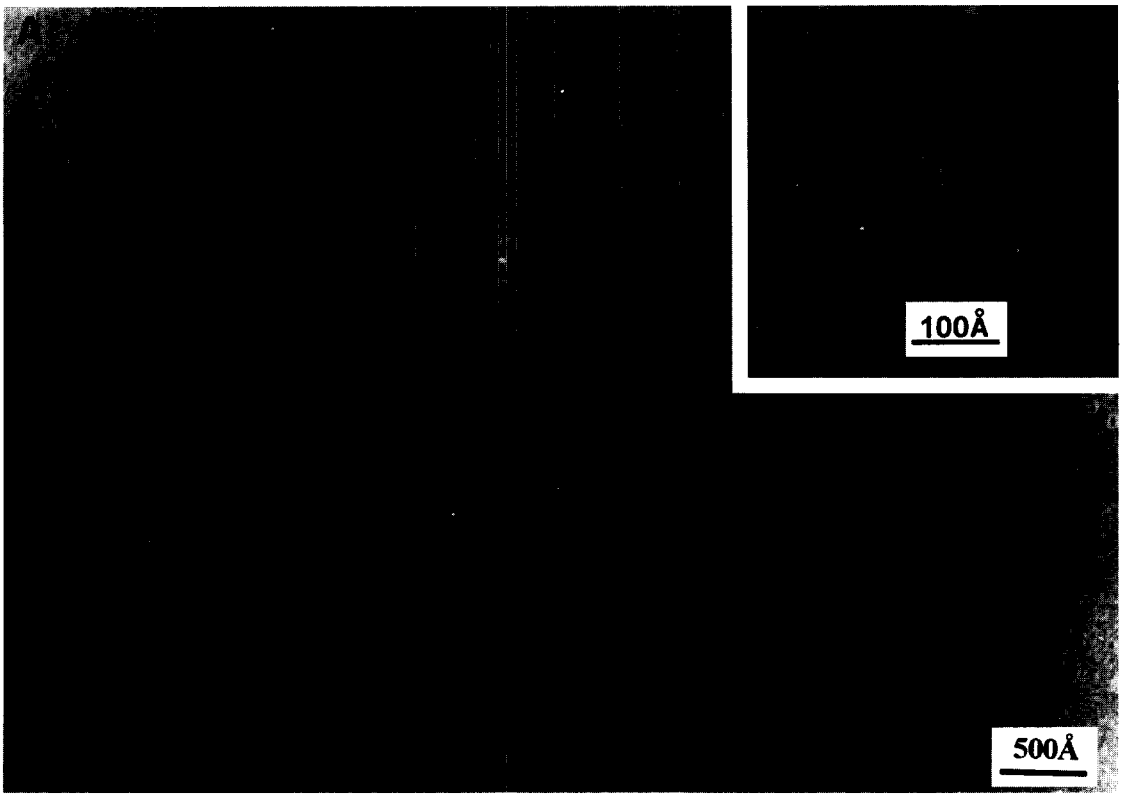

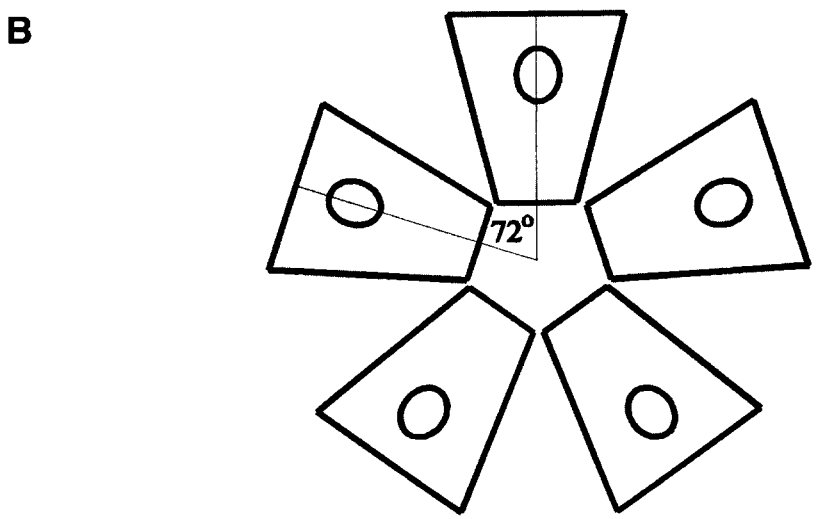

Fig. 5. Electron micrograph of the dispersed oligomeric CRP molecules on DS8PE/DOPC (1:5) monolayer and an assembling model of the oligomeric CRP. (A) Electron micrograph of a negatively stained specimen. It was taken at 100 000× with an operation voltage of 100 kV. Insert: the individual ring structure of oligomeric CRP printed at higher magnification. (B) A model of the pentameric structure of the oligomeric CRP molecule.

cific binding-induced 2D crystal is the top view, and that in the non-specific adsorption-induced 2D crystals is a side view. The top and the bottom of the trapezoid monomers in the specific binding-formed 2D crystals (Fig. 3C) correspond to the small and large end of the elliptical monomers in the non-specific adsorption-formed 2D crystals (Fig. 4C) separately. These two projection maps both have a length of 60 Å along the major axis, and both have a region of stain-excluding protein (marked with ★ in Figs. 3C and 4C), which are both about 20 Å away from the extreme of the large end. We suggest that this region may be the structural center of the monomer. In the projection map of the monomer of the specific binding-induced 2D crystals, the density decreases more sharply from the center to the bottom than that to the top side (Fig. 3C). This reflects the mass density variations of the protein lying in the plane vertical to the incident electron beam, and it coincides well with the variations of the monomer in the non-specific adsorption-formed 2D crystals in breadth of the outline (Fig. 4C).

Pentameric structures are relatively rare configurations for

proteins [50]. Theoretically, the monomers in an oligomeric macromolecule could be assembled in a variety of different geometries that depend on the saturation of the interface bonding potentials and the environment of each of the monomers. If each of the monomers of the oligomer is in an identical environment and if the bonding potential of the monomers is saturated, then the only possible arrangement of a pentamer is cyclic symmetry [50], with the monomers arranged at the corners of a pentagon. Indeed, the structure of the rabbit CRP shows a cyclic pentamer. With the sizes of both the oligomer and the monomer of CRP obtained in our experiments as mentioned above, we propose a model of the oligomeric CRP (see Fig. 5B). The model in Fig. 5B is an overview. Facing towards the membrane surface in an identical way, the five monomers are positioned at the corners of the planar pentagon forming a ring. The small top sides of the monomers are towards to the center of the ring. In this arrangement the diameter of the ring is about 135 Å, and that of the central cavity is about 30 Å, which agrees with the electron microscopic data of the oligomeric CRP (Fig. 5A).

CRP exists as a pentamer in the serum, but it only crystallizes in 2D as monomers in the present work. Further study is needed to explain the reason for the disaggregation.

Acknowledgements: We are grateful to Dr. Da-Neng Wang and Dr. Jonathan Boulter (Skirball Institute of Biomolecular Medicine, New York University Medical Center) for critical reading of the manuscript.

References

[1] Tillet, W.S. and Francis, T. (1930) J. Exp. Med. 52, 561–571.
[2] Kushner, I. (1982) Ann. NY Acad. Sci. 389, 1157–1165.
[3] Gewurz, H., Mold, C., Siegel, J. and Fiedel, B. (1982) Adv. Int. Med. 27, 345–372.
[4] Kaplan, M.H. and Volanakis, J.E. (1974) J. Immunol. 112, 2135–2147.
[5] Siegel, J., Rent, R. and Gewurz, H. (1974) J. Exp. Med. 140, 631–647.
[6] Kindmark, C.-O. (1971) Clin. Exp. Immunol. 8, 941–948.
[7] Fiedel, B.A., Simpson, R.M. and Gewurz, H. (1982) Immunology 45, 439–447.
[8] James, K., Hansen, B. and Gewurz, H. (1981) J. Immunol. 127, 2539–2544.
[9] James, K., Hansen, B. and Gewurz, H. (1981) J. Immunol. 127, 2545–2550.
[10] Abernathy, T.J. and Avery, O.T. (1941) J. Exp. Med. 73, 173–190.
[11] Volanakis, J.E. and Kaplan, M.H. (1971) Proc. Soc. Exp. Biol. Med. 136, 612–614.
[12] Gotschlich, E.C. and Edelman G.M. (1967) Proc. Natl. Acad. Sci. USA 57, 706–712.
[13] Soelter, J. and Uhlenbruck, G. (1986) Immunology 58, 139–144.
[14] Osmand, A.P., Friedenson, B., Guwurz, H., Painter, R.H., Hofmann, T. and Shelton, E. (1977) Proc. Natl. Acad. Sci. USA 74, 739–743.
[15] Olivera, E.B., Gotschlich, E.C. and Liu, T.-Y. (1979) J. Biol. Chem. 254, 489–502.
[16] Woo, P., Kornberg, J.R. and Whitehead, A.S. (1985) J. Biol. Chem. 260, 13384–13390.
[17] Lei, K.-J., Liu, T., Zon, G., Soravia, E., Liu, T.-Y. and Goldman, N.D. (1985) J. Biol. Chem. 260, 13377–13383.
[18] Liu, T.-Y., Syin, C., Nguyen, N.Y., Suzuki, A., Boykins, R.A., Lei, K.-J. and Goldman, N. (1987) J. Protein Chem. 6, 263–272.
[19] Volanakis, J.E. and Kearney, J.F. (1981) J. Exp. Med. 153, 1604–1614.
[20] Vasta, G.R., Marchalonis, J.J. and Kohler, H. (1984) J. Exp. Med. 159, 1270–1276.
[21] Pepys, M.B. and Baltz, M.L. (1983) Proc. Natl. Acad. Sci. USA 74, 739–743.
[22] Myles, D.A.A., Bailey, S., Rule, S.A., Jones, G.R. and Greenhough, T.J. (1990) J. Mol. Biol. 213, 223–225.
[23] Hopkins, M., Flanagan, P.A., Bailey, S., Glover, I.D., Myles, D.A.A. and Greenhough, T.J. (1994) J. Mol. Biol. 235, 767–771.
[24] DeLucas, L.J., Greenhough, T.J., Rule, S.A., Myles, D.A.A., Babu, Y.S., Volanakis, J.E. and Bugg, C.E. (1987) J. Mol. Biol. 196, 741–742.
[25] Myles, D.A.A., Rule, S.A., DeLucas, L.J., Babu, Y.S., Xu, Y., Volanakis, J.E., Bugg, C.E., Bailey, S. and Greenhough, T.J. (1990) J. Mol. Biol. 216, 491–496.
[26] Amos, L.A., Henderson, R. and Unwin, P.N.T. (1982) Prog. Biophys. Mol. Biol. 39, 183–231.
[27] Uzgiris, E.E. and Kornberg, R.D. (1983) Nature 301, 125–129.
[28] Kornberg, R.D. and Darst, S.A. (1991) Curr. Opin. Struct. Biol. 1, 642–646.
[29] Darst, S.A., Ribi, H.O., Pierce, D.W. and Kornberg, R.D. (1988) J. Mol. Biol. 203, 269–273.
[30] Darst, S.A., Kubalek, E.W. and Kornberg, R.D. (1989) Nature 340, 730–732.
[31] Darst, S.A., Ahlers, M., Meller, P.H., Kubalek, E.W., Blankenburg, R., Ribi, H.O., Ringdorf, H. and Kornberg, R.D. (1991) Biophys. J. 59, 387–396.
[32] Ludwig, D.S., Ribi, H.O., Schoolnik, G.K. and Kornberg, R.D. (1986) Proc. Natl. Acad. Sci. USA 83, 8585–8588.
[33] Newman, R., Tucker, A., Ferguson, C., Tsernoglou, D., Leonard, K. and Crumpton, M.J. (1989) J. Mol. Biol. 206, 213–219.
[34] Ribi, H.O., Ludwig, D.S., Mercer, K.L., Schoolnik, G.K. and Kornberg, R.D. (1988) Science 239, 1272–1276.
[35] Ribi, H.O., Reichard, P. and Kornberg, R.D. (1987) Biochemistry 26, 7974–7979.
[36] Robinson, J.P., Schmid, M.F., Morgan, D.G. and Chiu, W. (1988) J. Mol. Biol. 200, 367–375.
[37] Uzgiris, E.E. (1986) Biochem. Biophys. Res. Commun. 134, 819–826.
[38] Qin, H., Liu, Z. and Sui, S.F. (1995) Biophys. J. 68, 2493–2496.
[39] Anderson, H.C. and McCarty, M. (1951) J. Exp. Med. 93, 25–36.
[40] Swanson, S.J. and Mortensen, R.F. (1990) Mol. Immunol. 27, 679–687.
[41] Liu, Z., Sui, S.F., Gao, Q.F. and Zhou, Q.Z. (1995) Acta Biophys. Sin. 11, 201–208.
[42] Diembeck, W. and Eibl, H, (1979) Chem. Phys. Lipids 24, 237–244.
[43] Eibl, H. and Nicksch, A. (1978) Chem. Phys. Lipids 22, 1–8.
[44] Mosser, G. and Brisson, A. (1991) J. Struct. Biol. 106, 191–198.
[45] Mosser, G., Mallouh, V. and Brisson, A. (1992) J. Mol. Biol. 226, 23–28.
[46] Ou, S.H., Mann, J.A., Lando, J.B., Zhou, L. and Singer, K.D. (1992) Appl. Phys. Lett. 61, 2284–2286.
[47] Henderson, R., Baldwin, J.M. and Ceska, T.A. (1990) J. Mol. Biol. 213, 899–929.
[48] Volanakis, J.E. and Wirtz, K.W.A. (1979) Nature 281, 155–157.
[49] Roux, K.H., Kilpatrick, J.M., Volankis, J.E. and Kearney, J.F. (1983) J. Immun. 131, 2411–2415.
[50] Klotz, I.M., Darnall, D.W. and Langerman, N.R. (1975) in: The Protein (Neurath, H. and Hill, R.L., Eds.) 3rd edn., Vol. 1, pp. 293–411. Academic Press, New York.